Spatial and temporal assessment of organic and black carbon at four sites in the interior of South Africa

Petra Maritz[1], Johan P. Beukes[1], Pieter G. van Zyl[1,*], Elne H. Conradie[1], Catherine Liousse[2], Corinne Galy-Lacaux[2], Pierre Castéra[2], Avishkar Ramandh[3], Gabi Mkhatshwa[4], Andrew D. Venter[1] and Jakobus J. Pienaar[1]

[1]Unit for Environmental Sciences and Management, North-West University, Potchefstroom Campus, Private Bag X6001, Potchefstroom, 2520, South Africa, 20229143@nwu.ac.za, Paul.Beukes@nwu.ac.za, Pieter.VanZyl@nwu.ac.za, 12407690@nwu.ac.za, 20049544@nwu.ac.za , Kobus.Pienaar@nwu.ac.za

[2]Laboratoire d'Aérologie, Université Paul Sabatier-CNRS, OMP, 14 Avenue Edouard Belin, 31400 Toulouse, France. Cathy.Liousse@aero.obs-mip.fr, corinne.galy-lacaux@aero.obs-mip.fr

[3]Sasol Technology R&D, P.O Box 1183, Sasolburg, 1947, South Africa, Avishkar.Ramandh@sasol.com

[4]Sustainability & Innovation Department, Eskom Corporate Service Division, Rosherville, South Africa. Gabi.Mkhatshwa@eskom.co.za

*Corresponding author. Tel. +2718 99 23 53; E-mail address: Pieter.VanZyl@nwu.ac.za (P.G. van Zyl)

Abstract

Limited data currently exist for atmospheric organic carbon (OC) and black carbon (BC) in South Africa (SA). In this paper OC and BC measured in SA were explored in terms of spatial and temporal patterns, mass fractions of the total aerosol mass, as well as possible sources. PM_{10} and $PM_{2.5}$ samples were collected at five sites in SA operated within the Deposition of Biogeochemical Important Trace Species-IGAC DEBITS in Africa (DEBITS-IDAF) network. OC were higher than BC concentrations at all sites in both size fractions, while most OC and BC occurred in the $PM_{2.5}$ fraction. OC/BC ratios reflected the location of the different sites, as well as possible sources impacting these sites. The OC and BC mass fraction percentages of the total aerosol mass varied up to 24% and 12%, respectively. A relatively well defined seasonal pattern was observed, with higher OC and BC measured from May to October, which coincides with the dry season in the interior of SA. An inverse seasonal pattern was observed for the fractional mass contributions of OC and BC to the total aerosol mass, which indicates substantially higher aerosol load during this time of the year. The relationship between OC and BC concentrations with the distance that air mass back trajectories passed by biomass burning fires and large point sources proved that biomass burning fires contribute significantly to regional OC and BC during the burning season, while large point sources did not contribute that significantly to regional OC and BC. The results from a highly industrialised and populated site also indicated that household combustion for space heating contributed at least to local OC and BC concentrations.

Keywords

Black carbon (BC), Organic carbon (OC), Spatial, Temporal, DEBITS, IDAF

Introduction

Atmospheric aerosols have impacts on climate change and general air quality, which are determined by their physical (size, mass, structure, concentration and optical density) and chemical properties (Seinfeld and Pandis 2006). Typical chemical species present in atmospheric aerosols include wind-blown dust particles (e.g. pollen, bacteria, smoke, ash, sea salt), black carbon (BC), organic carbon (OC), sulphates (SO_4^{2-}) nitrates (NO_3^-), ammonium (NH_{4+}) and trace metal species. Aerosols are generally classified according to their size, e.g. PM_{10} (aerodynamic diameter ≤ 10 μm), $PM_{2.5}$ (aerodynamic diameter ≤ 2.5 μm), PM_1 (aerodynamic diameter ≤ 1 μm) and $PM_{0.1}$ (aerodynamic diameter ≤ 0.1 μm) particulates (Slanina

and Zhang 2004; Pöschl 2005). The baseline of uncertainty in aerosol radiative forcing is large and depends on the afore-mentioned aerosol characteristics, which can vary significantly on a regional and global scale (Slanina and Zhang 2004; IPCC 2013). General detrimental effects of atmospheric aerosol pollution on human health include increased cardiopulmonary and respiratory diseases (Gauderman et al. 2004), while $PM_{0.1}$ can even diffuse through the membranes of the respiratory track into the blood stream (Oberdörster et al. 2004; Pöschl 2005). Environmental impacts of atmospheric aerosol pollution include acid deposition and eutrophication (Lazaridis et al. 2002; Pöschl 2005).

Atmospheric BC is emitted as a primary species, while OC can consist of primary and secondary aerosols (Putaud et al. 2004; Pöschl 2005). Major sources of BC and OC include incomplete combustion of fossil fuels, biomass burning and traffic emissions (Bond and Sun, 2005; IPCC 2013). OC is also emitted from biogenic sources and can be formed through the oxidation of volatile organic compounds (VOCs) (Pöschl 2005). BC absorbs terrestrial long-wave radiation that has a warming effect on the atmosphere, while OC, depending on their chemical properties, could absorb or reflect incoming solar radiation (IPCC 2013).

In general it is accepted that OC has a net cooling effect (IPCC 2013). After CO_2, BC is considered to be the second most important contributor to global warming (Bond and Sun 2005; IPCC 2013). The impacts of BC are especially significant on local and regional scales, since BC has a relatively short atmospheric lifetime (days to weeks) (IPCC 2013). Greenhouse gases (GHG) spend much longer periods in the atmosphere, i.e. between 10 to 100 years (de Richter and Caillol 2011).

Although Africa is regarded as the largest source region of anthropogenic atmospheric OC and BC (Liousse et al. 1996; Kanakidou et al. 2005), it is one of the least studied continents. Within Africa, southern Africa is an important source region. Biomass burning fires (anthropogenic and natural) are endemic across this region especially during the dry season when almost no precipitation occurs (Formenti et al. 2003; Tummon et al. 2010; Laakso et al. 2012).

Biomass burning fire plumes from southern Africa are known to impact Australia and South America (Swap et al. 2004). In addition, South Africa is the economic and industrial hub of southern Africa with large anthropogenic point sources (e.g. Lourens et al. 2011). However, the relative importance of OC and BC contributions from these anthropogenic sources in Africa are still largely unknown, although some papers have been published that considered sources in west African capitals (Doumbia et al. 2012; Val et al. 2013). Venter et al. (2012) used BC data that were collected at Marikana in the North West province (South Africa) to verify that the origin of CO and PM_{10} was related to BC, while Collett et al. (2010) only presented a single diurnal plot for BC measured at Elandsfontein in the Mpumalanga Highveld. Hyvärinen et al. (2013) used BC data collected at Welgegund in the North West province to illustrate the use of a newly developed method to correct BC values measured with a multi-angle absorption photometer (MAAP), but did not go into further detail of the BC data.

Within the framework of the Deposition of Biogeochemical Important Trace Species (DEBITS)-International Global Atmospheric Chemistry (IGAC) DEBITS in Africa (IDAF) project (Galy-Lacaux et al. 2003; Martins et al. 2007), atmospheric gaseous and aerosol measurements have been performed continuously since 1994 at 7 sites in central and western Africa, as well as 3 sites in South Africa. Regarding carbonaceous aerosol, Martins (2009) determined BC and OC concentrations at two of the South African IDAF sites. However, these measurements

were restricted to three two-week winter campaigns and one two-week summer campaign. This data have also not yet been published in the peer reviewed scientific domain.

In order to address the current knowledge gap, i.e. very limited OC and BC data for South Africa the main objectives of this paper are to present spatial and temporal assessments of OC and BC concentrations at the South African IDAF sites, determine the mass fractions of OC and BC of the overall aerosol mass, as well as to determine possible sources.

Experimental

Sampling sites

Aerosol samples were collected at five sampling sites in South Africa operated within the IDAF network, i.e. Louis Trichardt (LT), Skukuza (SK), Vaal Triangle (VT), Amersfoort (AF) and Botsalano (BS). The locations of these sites within a regional context are presented in Fig. 1. The South African IDAF sites are located in the north eastern part of the interior of South Africa. Mphepya et al. (2006) and Martins et al. (2007) have previously introduced LT and SK, but not the other sites. In order to contextualise all the sites a short description of each site is given in Table 1. LT, SK and BT are considered to be background sites.

In contrast, AF lies southeast of the internationally well-known NO_2 hotspot that is clearly visible from satellite observations over the Mpumalanga Highveld of South Africa (Lourens et al. 2012), while VT lies within a highly industrialised and populated area that has been proclaimed a national air pollution hotspot in terms of the South African National Environmental Management Act: Air Quality (Government Gazette Republic of South Africa 2005). Although not specified in Table 1, all the South African IDAF sites are likely to be impacted by local, as well as regional biomass burning fire emissions.
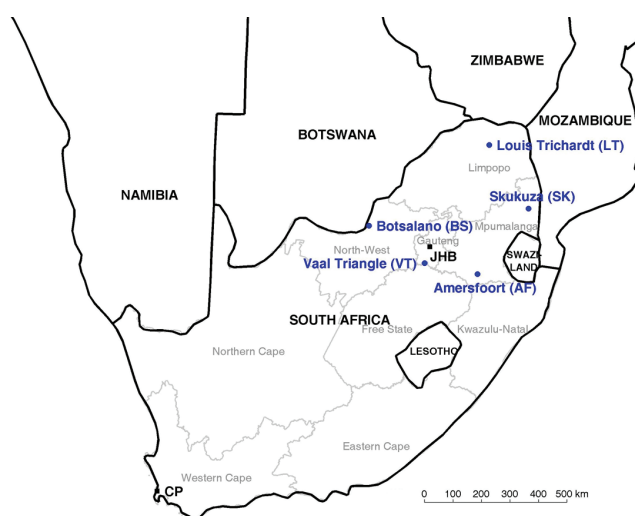
Figure 1: *The location (blue dots) of the South African IDAF sampling sites where OC and BC measurements were conducted are indicated on a southern African map. Provincial borders with the provincial names within South Africa, as well as Johannesburg (JHB) and Cape Town (CP) are also included for reference*

Table 1: Geographic coordinates and short descriptions of South African IDAF sampling sites where OC and BC measurements were conducted

Site	Location	Description
Amersfoort (AF)	27˚04'13"S 29˚52'02"E, 1628 m amsl	Semi-arid, within grassland biome, impacted by anthropogenic activities on the Mpumalanga Highveld
Louis Trichardt (LT)	22˚59'10"S 30˚01'21"E, 1300 m amsl	Semi-arid, within savannah biome, rural site predominantly used for agricultural purposes
Skukuza (SK)	24˚59'35"S 31˚35'02"E, 267 m amsl	Semi-arid, within savannah biome, regional background site in a protected area (Kruger National Park)
Vaal Triangle (VT)	26°43'29"S 27°53'05"E, 1320 m amsl	Semi-arid, within grassland biome, situated in the highly industrialized Vaal Triangle area, impacted by emissions from various industries, traffic and household combustion
Botsalano (BS)	25 32'28"S, 25 45'16"E	Semi-arid, within savannah biome, regional background site in a protected area (Botsalano Game Reserve)

Regional meteorology

Recently Laakso et al. (2012) and references therein gave an overview of the meteorology over the South African Highveld, as well as the interaction between meteorological patterns and pollutant levels. Therefore only a synopsis is presented here. Atmospheric circulation over the South African Highveld is dominated by an anti-cyclonic recirculation pattern throughout the year (Tyson and Preston-Whyte 2000), due to the dominance of a continental high pressure cell over the interior. This recirculation contributes significantly to the build-up of pollutants. This is especially significant during the cold dry winter (June – August) and early spring months (September – middle October) when strong inversion layers trap pollutants at several different heights inhibiting vertical mixing. This frequently causes an increase in atmospheric pollutant concentrations near the surface. In addition, the interior of South Africa is also characterised by a distinct wet and dry season. Almost all the precipitation occurs during the wet season from middle October to April, while nearly no precipitation takes place during the dry season from May to middle October. The lack of precipitation during the dry season leads to a decrease in wet deposition of pollutants and indirectly to the increase in pollutant levels due to the more frequent occurrence of large scale biomass burning fires. During the cooler autumn and cold winter months (May to August) household combustion for space heating is also a common occurrence in especially semi-formal and informal settlements (Venter et al. 2012).

Sampling

One 24-hour $PM_{2.5}$ and one PM_{10} aerosol sample was collected on quartz filters (with a deposit area of 12.56 cm^2) once a month from March 2009 to April 2011 at each site. A total of 258 samples

were collected, i.e. 52 samples for each site, except for BS for which only 50 samples were collected. Since both size fractions were sampled each month at each site, one half of the samples were $PM_{2.5}$ and the other half PM_{10}. The quartz filters were prebaked at 900°C for 4 hours and cooled down in a desiccator, prior to sample collection. MiniVol samplers developed by the United States Environmental Protection Agency (US-EPA) and the Lane Regional Air Pollution Authority were used during sampling (Baldauf et al. 2001). These samplers have a pump that is controlled by a programmable timer, which allows for the collection of samples at a constant flow rate over a pre-determined time period. In this study, samples were collected at a flow rate of 5 L/min, which was verified by using a handheld flow meter that was supplied with the MiniVol samplers. Filters were handled with tweezers while wearing surgical gloves, as a precautionary measure to prevent possible contamination of the filters. All thermally pre-treated filters were also visually inspected to ensure that there were no weak spots or flaws. After inspection, acceptable filters were weighed and packed in airtight Petri dish holders until they were used for sampling. After sampling, the filters were again placed in Petri dish holders, sealed off, bagged and stored in a portable refrigerator for transport to the laboratory. At the laboratory the sealed filters were stored in a conventional refrigerator. 24 hours prior to analysis, samples were removed from the refrigerator and weighed just prior to analysis.

OC and BC Analysis

Several methods can be used to analyse OC and BC collected on filters (Chow et al. 2001). It was decided to apply the IMPROVE thermal/optical (TOR) protocol (Chow et al. 1993; Chow et al. 2004; Environmental analysis facility 2008; Guillaume et al. 2008) by using a Desert Research Institute (DRI) thermal optical carbon analyser. In this method, filters are submitted to volatilization at temperatures of 120, 250, 450 and 550°C in a pure Helium (He) atmosphere and thereafter to combustion at temperatures of 550, 700 and 800°C in a mixture of He (98%) and oxygen (O_2) (2%) atmosphere. The carbon compounds that are released are then converted to CO_2 in an oxidation furnace with a manganese dioxide (MnO_2) catalyst at 932°C. Then, the flow passes into a digester where the CO_2 is reduced to methane (CH_4) on a nickel-catalysed reaction surface. The amount of CH_4 formed is detected by a flame ionization detector (FID), which is converted to carbon mass using a calibration coefficient. The carbon mass peaks detected correspond to the different temperatures at which the seven separate carbon fractions, which include four OC and three BC fractions, were released. These fractions were depicted as different peaks on the thermogram, of which the surface areas were proportional to the amount of CH_4 detected. The reflectance from the deposited sample is monitored throughout the afore-mentioned analysis. This reflectance usually decreases during the volatilization process due to the pyrolysis of OC. When oxygen is added, the reflectance is increased as the BC is burnt and removed. OC is defined as the fraction which evolves prior to re-attainment of the original reflectance (the non-absorbing light particles) and BC is defined as the fraction which evolved after the original reflectance

has been attained (the light absorbing particles). The DRI instrument can detect OC and BC as low as 0.1 μg/cm².

Back trajectory analysis

Back trajectories of air masses were calculated with the Hybrid Single-Particle Lagrangian Integrated Trajectory (HYSPLIT 2014) model (version 4.8), developed by the National Oceanic and Atmospheric Administration (NOAA) Air Resources Laboratory (ARL) (Draxler and Hess 2004). This model was run with meteorological data of the GDAS archive of the National Centre for Environmental Prediction (NCEP) of the United States National Weather Service and archived by the ARL (Air Resources Laboratory 2014a), which has a 40 or 80 km grid resolution, depending on the actual year considered (Nasa 2015). The HYSPLIT model computes air trajectories, as well as more complicated dispersion and deposition simulations. This model uses the Lagrangian- and the Eulerian approach. The Lagrangian approach uses a moving frame as the air particles move from their original location. The Eulerian approach uses a fixed three-dimensional grid as frame. The Lagrangian framework follows the transport of the air particles, while the Eulerian approach calculates the pollutant concentrations on a fixed grid. The Hysplit model is mainly used for tracking and forecasting the release of different pollutants (e.g. radioactive material, volcanic ash, wildfire smoke) from stationary or mobile emission sources (Air Resources Laboratory 2014b).

All back trajectories were calculated for 24 hours, arriving on the hour at a height of 100 m above ground level at each of the sites presented in Table 1. Although a number of uncertainties have to be taken into account when working with the HYSPLIT data (Air Resources Laboratory 2014c), the most relevant here was the spatial complexity of the area. Therefore, an arrival height of 100 m was chosen, since the orography in HYSPLIT is not very well defined, which could results in increased error margins on individual trajectory calculations if lower arrival heights were used. For back trajectories calculated in this manner, maximum error margins of 15 to 30% of the trajectory distance travelled have been reported (Stohl 1998; Riddle et al. 2006; Vakkari et al. 2011).

Correlation between back trajectory analysis and sources

In this study back trajectory analysis of air masses was employed to relate BC and OC concentrations measured at a specific sampling site with the closest distance between the trajectory calculated for a specific 24-hour sampling period and biomass burning fire events occurring during that time, as well as large point sources. Although a number of products can be used to obtain biomass combustion fire locations, the fire locations used in this paper were obtained from the remote sensing observations of fires from the MODIS collection 5 burned area product (Roy et al. 2008; MODIS 2014). Since MODIS burned area observations are obtained from a satellite passing over an area once a day, the 24-hour back trajectories were calculated to arrive at the middle of each 24-hour sampling period. Fig. 2 presents an illustration of the method applied for a specific

sampling site to determine the shortest distance between a 24-hour back trajectory and burned areas identified within the period correlating closest to the sampling period. The distances between burned areas (indicated by the red areas) and a specific back trajectory were calculated for each of the hourly locations of the 24-hour back trajectory (indicated by the blue dots in Fig. 2). In the example presented here (Fig. 2), the symbol A indicates the shortest distance between hourly locations of this specific trajectory and burned areas. Similar calculations were made to determine the shortest distance that the afore-mentioned back trajectories had passed large point sources. In the graphical example presented here (Fig. 2), symbol B indicates the shortest distance between hourly locations of this specific trajectory and large point sources (i.e. petrochemical operations, coal-fired power stations and pyrometallurgical smelters) in the north-east of South Africa. Similar calculations were performed for each OC and BC sampling period, where after OC and BC levels were plotted against the shortest distances between back trajectory paths and fire events/large point sources for all days at all sites. Weakness of the afore-mentioned method were that downwind fires, very close to the monitoring site, could in some instances be the closest fire(s) and that dilution due to distance travelled by the trajectories were not considered.
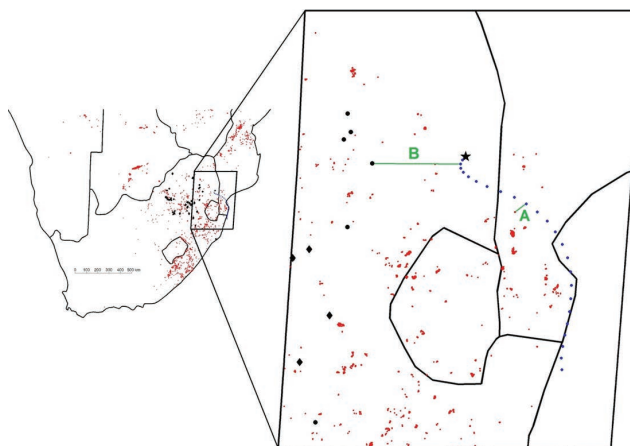
Figure 2: *Example to illustrate the method applied to determine the shortest distance between 24-hour back trajectories and burned areas, as well as large point sources. The red areas indicate burned areas identified by the MODIS collection 5 burned area product on a specific overpass, the black markers large point sources (circles indicating pyro-metallurgical smelters and diamonds representing coal-fired power stations), while the blue dots represent the hourly locations of the example 24-hour back trajectory calculated for Skukuza (indicated by the black star). Symbol A indicates shortest distance between the trajectory and a burned area, while symbol B indicates the shortest distance that the back trajectory had passed a large point source.*

Results and discussion

Spatial assessment

In Fig. 3a and Fig. 3b box and whisker plots of the concentrations of OC and BC measured, in the PM$_{2.5}$ (a) and PM$_{10}$ (b) size fractions at each of the sites for the entire sampling period, is presented, with OC/BC ratios also indicated.
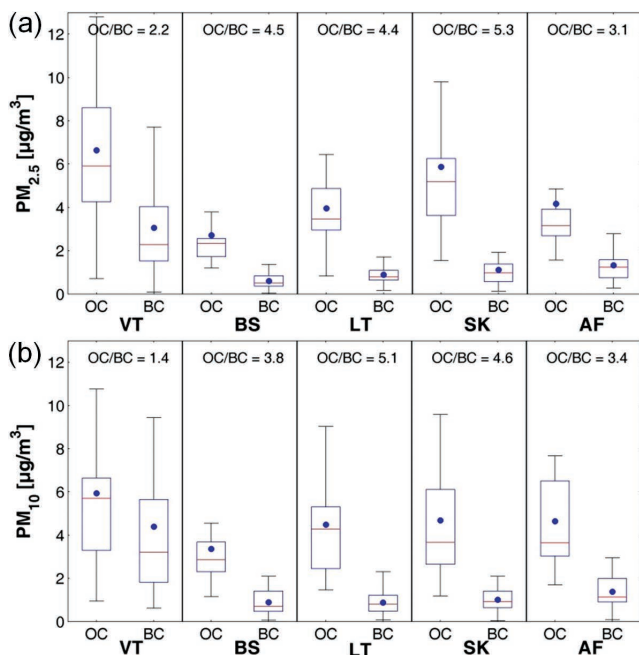
Figure 3: *Statistical distribution of PM$_{2.5}$ (a) and PM$_{10}$ (b) OC and BC measured at the various South African IDAF sites. The line in each box indicates the median, the dot the mean, the top and bottom edges of the box the 25th and 75th percentiles and the whiskers ± 2.7 σ(99.3% coverage if the data has a normal distribution). The average OC/BC ratio for every site is also shown*

From Fig. 3 it is evident that OC concentrations were higher than BC levels at all the South African IDAF sites in the PM$_{2.5}$ (3a) and PM$_{10}$ (3b) fractions. In general OC and BC concentrations in both size fractions were the highest at VT, with especially the BC levels being much higher compared to the other sampling sites. Therefore the OC/BC ratios of VT, i.e. 2.2 (PM$_{2.5}$) and 1.4 (PM$_{10}$), were also significantly lower than for the other sites. AF had the second lowest OC/BC ratio, i.e. 3.1 (PM$_{2.5}$) and 3.4 (PM$_{10}$), whereas the OC/BC ratios varied between 3.8 and 5.3 for the remaining sites. The reason for the higher OC and BC levels and the lower OC/BC ratio for VT can be ascribed to its location that is much different compared to the other sites. The VT is situated in an area where most of the South African petrochemical and related chemical industries are located, together with other large point sources that include two coal-fired power stations and numerous metallurgical smelters (Beukes et al. 2013). This area is also densely populated with large semi-formal and informal settlements. Venter et al. (2012) recently reported that the dominant source of PM$_{10}$ measured at a site in a highly industrialised region in South Africa, with numerous semi- and informal settlements in close proximity, was household combustion. This indicates that household combustion for space heating and cooking in these settlements in the VT area could also be a significant source of OC and BC. Higher traffic volumes in this densely populated area will also contribute to OC and BC concentrations. Less dilution of BC and lower secondary formed OC due to the close proximity to the sources also contribute to the different observation at the VT site.

The OC concentrations at LT, SK and AF were in the same range in the PM$_{10}$ fraction, while slightly higher OC levels were measured at SK in the PM$_{2.5}$ fraction compared to LT and AF. The lowest OC concentrations were measured at BS. The BC concentrations at BS, LT, SK and AF were in the same order in the PM$_{10}$ and PM$_{2.5}$ fractions throughout the sampling period, although BC levels were slightly higher at the anthropogenically impacted AF (Table 1). LT, SK and BS are regarded as background sampling sites (Table 1).

It is also evident from Fig. 3 that most of the OC and BC species measured were in the PM$_{2.5}$ fraction, since OC and BC concentrations in the PM$_{2.5}$ fraction did not differ significantly compared to OC and BC concentrations in the PM$_{10}$ fraction that also included PM$_{2.5}$ particulates. This indicates that the major sources of OC and BC are anthropogenic activities e.g. incomplete combustion of fossil fuels and household combustion, as well as biomass combustion fires that can be natural and anthropogenic in South Africa (Vakkari et al. 2014). An anomaly in the data was that the OC levels measured at VT were higher in the PM$_{2.5}$ fraction than in the PM$_{10}$ fraction, which cannot be possible. This can be attributed to an artefact in the sampling method utilised. As described in the experimental section, PM$_{10}$ and PM$_{2.5}$ samples were collected for the same sampling period with two separate MiniVol samplers with flows being checked prior and after sampling. Although no deviations were observed from the set point flow, it is possible that the sampling flow rate of 5 L/min was not maintained constantly in a single, or a small number of measurements, resulting in differences in sampling volumes. However, this anomaly was not present for any of the other sites. Additionally, the anomaly observed for the VT site does not detract from the conclusion made for all the sampling sites that the both OC and BC occurred mostly in the smaller size fraction, i.e. PM$_{2.5}$.

As previously mentioned, the OC/BC ratios of VT were significantly different compared to the other sites. However, it can also be stated that the OC/BC ratio of AF, i.e. 3.1 (PM$_{2.5}$) and 3.4 (PM$_{10}$), is in-between that of the directly anthropogenic impacted VT and the background sites, i.e. BS, LT and SK. According to Junker and Liousse (2008) biomass burning fire and biofuel emissions usually have higher OC/BC ratios than fossil fuel sources. The calculated OC/BC ratios therefore indicate that VT is mostly influenced by fossil fuel sources, while BS, LT and SK are more significantly influenced by biomass burning fire emissions. Mphepya et al. (2006) and others (e.g. Formenti et al. 2003) have previously indicated that SK is significantly influenced by biomass burning fire emissions during the dry season. The in-between OC/BC ratios at AF indicate impacts from biomass burning fire and fossil fuel combustion emissions. The OC/BC ratios therefore reflect the location and possible sources impacting the different IDAF sites, as indicated in Table 1.

The OC/BC ratios at the South African IDAF sites compare well with those measured in other studies. Cachier et al. (2005) reported OC and BC measurements at five sites in France, i.e. Martigues, Marseilles, Réaltor, Plan d'Aups and Dupail. OC/BC ratios determined at Martigues and Marseilles, which are considered to be impacted by anthropogenic activities, were 2.16 and 2.07, respectively, while Réaltor that is slightly removed

from Martigues and Marseilles had an OC/BC ratio of 2.88. The OC/BC ratios for the two background sites, Plan d'Aups and Dupail, were 4.5 and 4.9, respectively. Chazette and Liousse (2001) determined an OC/BC ratio of 2.87 for Thessaloniki, which is the second biggest industrial city in Greece. Considering OC/BC ratio source characteristics proposed by Junker and Liousse (2008), it indicates that hard coal seems to be the dominant source type at VT, while typical OC/BC ratios associated with wood fuel, charcoal and motor gasoline correlated with OC/BC ratios determined at the other four South African IDAF sites. During SAFARI 2000, OC and BC samples were collected over the Atlantic Ocean just off the shore of Namibia and Angola from biomass burning fire plumes. The smoke of these biomass burning fires was widely distributed, and between one and two days old. In these samples the OC/BC ratios varied between 5.9 and 10.0 (Formenti et al. 2003). The higher OC/BC ratios reported by Formenti et al. (2003) can most likely be attributed to aging of the plumes and the absence of significant anthropogenic fossil fuel source contributions, which is also the case at the background South African IDAF sites, i.e. LT, SK and BS. Apart from the biomass burning fire emissions mentioned previously, these background sites are also influenced by re-circulating anthropogenic emissions from the South African Highveld.

As far as the authors could assess, the mass fractions of OC and BC as a function of the total aerosol mass, have not yet been investigated for South Africa. Therefore, in Fig. 4 box and whisker plots of the OC and BC mass fraction percentage of the total aerosol measured, in the $PM_{2.5}$ (4a) and PM_{10} (4b) size fractions, at each of the sites for the entire sampling period, are presented.
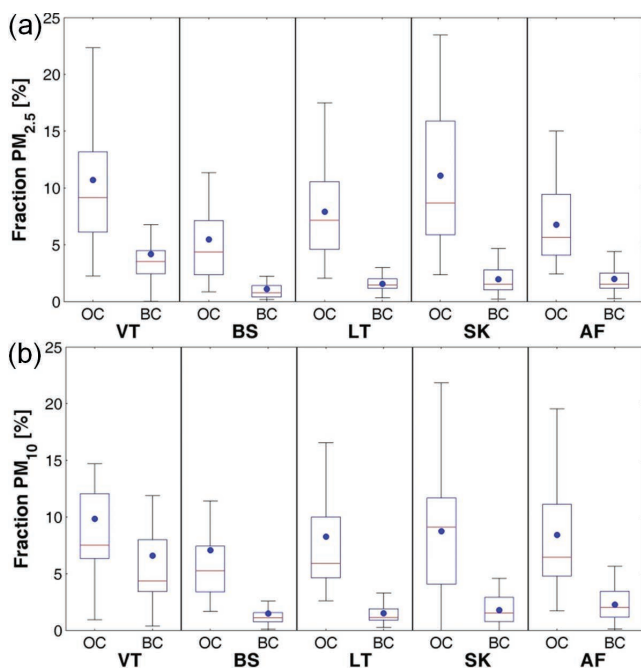
Figure 4: OC and BC as a mass fraction percentage of the total aerosol mass in $PM_{2.5}$ (a) and PM_{10} (b). The line in each box indicates the median, the dot the mean, the top and bottom edges of the box the 25th and 75th percentiles and the whiskers ± 2.7σ (99.3% coverage if the data has a normal distribution)

As expected, the OC mass fraction is higher than that of BC at all the sites for $PM_{2.5}$ and PM_{10}. The OC mass fraction percentage was up to 24%, while the BC mass fraction percentage was up to 12 % for all the sites in both size fractions. Putaud et al. (2004) reported $PM_{2.5}$ OC mass fractions to be 20-30% (rural sites) and 22-38% (near-city and kerbside sites), whereas PM_{10} OC mass fractions were 12-30% (rural sites) and 20-25% (near-city and kerbside sites) at 24 western European sites in winter. The BC contributions for $PM_{2.5}$ were reported to be 5-11% (rural sites) and 5-23% (near-city and kerbside sites), while the BC contributions for PM_{10} were 2-8% (rural sites) and 4-15% (near-city and kerbside sites). Yin et al. (2005) reported the OC mass fraction in Ireland for $PM_{2.5}$ as 30-40% (non-urban sites) and 10-30% (urban sites), while the PM_{10} OC mass fractions were 15-45% (non-urban sites) and 4-20% (urban sites). The $PM_{2.5}$ BC mass fractions were 25-30% (non-urban sites) and 8-10% (urban sites), while PM_{10} BC mass fractions were 12-22% (non-urban sites) and 3-5% (urban sites). From the afore-mentioned references it seems that the OC and BC measured at the South African IDAF sites were in the same order of magnitude, or lower than the mass fractions measured in western Europe. However, the study of Putaud et al. (2004) was biased towards winter, while all seasons are represented in the South African IDAF results. Additionally, fractional contribution to the overall aerosol load of sulphate has substantially decreased in first world countries where deSOx technology has been applied (Zhang et al. 2007). However, in South Africa sulphate is still the dominant aerosol species (Martins et al. 2007; Tiitta et al. 2014) since substantial deSOx technology have not yet been applied.

The OC mass fraction at SK and the BC mass fraction at VT were the highest in the $PM_{2.5}$ and PM_{10} size fractions. The high OC mass fraction at SK can be attributed to natural and anthropogenic sources. Mphepya et al. (2006) previously indicated the substantial impact of biomass burning fire emissions at SK. SK, LT and BS lies within the savannah biome (Mucina and Rutherford 2006), which emits more natural biogenic volatile organic compounds (BVOCs) than the Dry Highveld Grassland Bioregion wherein VT and AF lie (Mucina & Rutherford 2006). The atmospheric lifetime of BVOCs are mostly in the order of minutes to hours (Atkinson and Arey 2003), indicating that BVOCs can be transformed to less volatile species that could be collected as aerosols at sampling sites in close proximity of sources of BVOCs. In contrast, anthropogenic VOCs, which in general occur at higher concentrations than BVOCs in South Africa, have much longer atmospheric lifetimes (Jaars et al. 2014 and references therein), implying that the less volatile species are more likely to be formed further away from the source(s). SK also lies on the dominant path of air mass movement from the anthropogenic industrial hub of South Africa, which implies that primary emitted anthropogenic VOC species have enough time to oxidise to form less volatile secondary species that are measured in the OC fraction at SK. The BC high mass fraction at VT is due to this site being within a well-known anthropogenic source region as previously indicated and the nature of the sources occurring in this area.

Temporal assessment

As previously discussed, most of the OC and BC occurred in the PM$_{2.5}$ fraction, since there was not a significant difference between OC and BC concentrations in the PM$_{2.5}$ and PM$_{10}$ fractions (Fig. 3). Therefore only the PM$_{2.5}$ measurements are presented and discussed further in this paper. A statistically meaningful seasonal temporal assessment for OC and BC concentrations could not be performed for each individual sampling site, since only one 24-hour PM$_{2.5}$ sample was obtained for each month at each site – one day cannot be construed as being representative of an entire month. However, since all 5 the South African IDAF sites are within a region with similar meteorological conditions and seasonal patterns, the results obtained at all the sites for the 2 years and 1 month measurement period were combined and statistically evaluated. Such a monthly temporal presentation of data gives a regional, rather than a site specific temporal impression. Box and whisker plot was not deemed appropriate to present the temporal statistical distribution, since there were too few data points per month, i.e. between 10 and 15. In Fig. 5 scatter plots indicating averages and standard deviations of the monthly OC (5a) and BC (5b) concentrations measured in the PM$_{2.5}$ fractions for all the sites over the entire sampling period, are presented (indicated in blue). Additionally, the VT data was also excluded from the dataset used to present the temporal pattern, which is indicated in another colour (red) in Fig. 5. This was done, since it was previously pointed out that the OC/BC ratio of the VT was substantially different compared to the other sites (Fig. 3), due to the close proximity and the nature of large point sources near the VT site.

From the data (Fig. 5), a relatively distinct seasonal pattern is
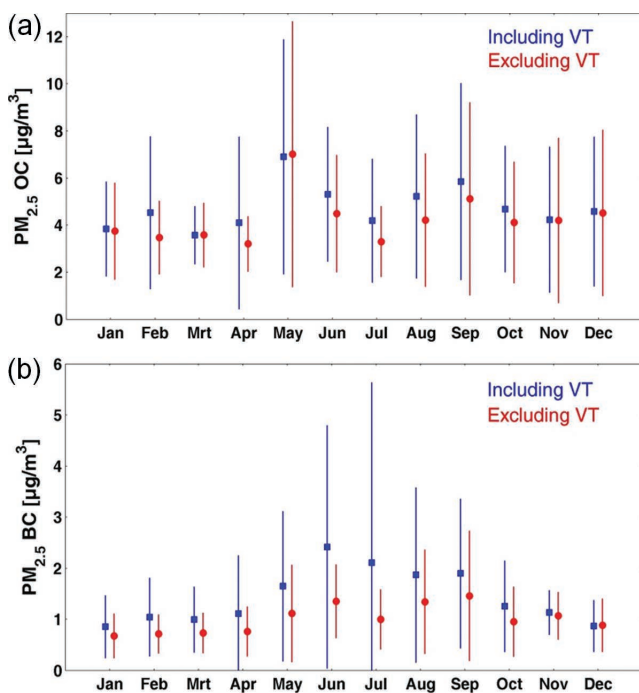
observed, with higher OC and BC concentrations generally occurring during the period from May to September with the only exception being the lower OC levels observed for July. This seasonal trend was true, irrespective if VT was included or excluded from the dataset (indicated with different colours in Fig. 5). The period with generally higher OC and BC levels (May to September in Fig. 5) coincide with the onset of the dry season that is typically from May to early October in the interior of South Africa. During the wet season (middle October to April) aerosols are more frequently removed from the atmosphere through wet deposition. Furthermore, the peak frequency of biomass combustion fires occurs during the dry period in southern Africa. Fire burning frequency is especially high during late winter and early spring, i.e. August and September in southern Africa. The period with generally higher OC and BC levels also coincide with the time of the year that persistent low-level inversion layers trap pollutants close to the surface (Laakso et al. 2012), which leads to an increase in atmospheric concentrations of pollutant species. The colder months (May to August) are additionally characterised by increased household combustion for space heating (Venter et al. 2012), which could lead to higher atmospheric OC and BC concentrations. The possible contributions of sources of OC and BC associated with the meteorological conditions, as well as the occurrence of biomass burning fire events will be explored later in the paper.
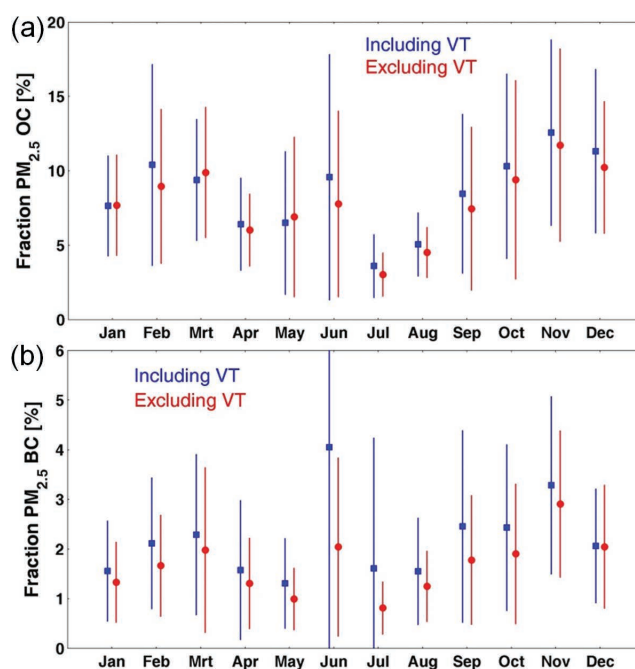
Figure 6: *Temporal variations of the average and standard deviation OC (a) and BC (b) mass fraction percentage in the PM$_{2.5}$ fraction at all the sampling sites (blue) and at all the sampling sites excluding VT (red) for the entire sampling period, i.e. March 2009 to April 2011*

In Fig. 6 temporal variations of the average and standard deviation OC (6a) and BC (6b) mass fractions of PM$_{2.5}$ for all the sites (including and excluding VT) over the entire sampling period are presented. With the exception of the OC and BC mass fractions of June, it is evident that the OC and BC seasonal mass fraction distribution (Fig. 6) is an inverse of the seasonal

Figure 5: *Temporal variations of the average and standard deviation of OC (a) and BC (b) concentrations in the PM$_{2.5}$ fraction at all the sampling sites (blue) and at all the sampling sites excluding VT (red) for the entire sampling period, i.e. March 2009 to April 2011*

OC and BC concentrations presented in Fig. 5. This indicates that although OC and BC concentrations are in general higher in the dry and cold period between May to August (Fig. 5), the atmospheric aerosol load during this period is also substantially higher, resulting in a lower fractional representation of OC and BC (Fig. 6). Unfortunately complete mass closure with all possible atmospheric aerosol species included could not be conducted during this study. Therefore it cannot be stated with certainty what other aerosol species are present in higher concentrations during May to August. However, it is likely that wind-blown dust concentrations will be higher during this time of the year, since less rainfall will result in higher wind-blown dust levels (Mphepya et al. 2004). Possible higher fractional sulphate content of aerosols in the dry season (Tiitta et al. 2014) could also contribute to the lower OC and BC mass fractions. Sulphate seems to be the dominant species in South African aerosols (Martins et al. 2007; Tiitta et al. 2014).

Possible sources of OC and BC

Although it seems obvious that biomass combustion fires contribute significantly to OC and BC concentrations, this was explored further. In Fig. 7 the frequency of biomass combustion fires (obtained from MODIS burned area measurements) from March 2009 to April 2011 (correlating to the sampling period in this study) are presented for southern Africa in the region between 15 – 35°S and 10 – 41°E. The numbers of fires within a 1000 km radius from the centre of the 5 IDAF sites are also indicated. From this data (Fig. 7) it is evident that the fires mainly occurred between June and October, which correlates with the seasonal pattern observed for OC and BC (Fig. 5). Furthermore, the highest frequency of fires occurred in August and September. The highest number of fire events recorded for southern Africa (15 – 35°S and 10 – 41°E) in a single month was approximately 1.2 million in September 2010. Roughly 550 000 of these biomass burning fire events took place within the 1000 km radius from the centre of the 5 IDAF sites.

As previously described, the distances calculated between back trajectories that arrived in the middle of each sampling period and biomass burning fire events recorded for the previous 24 hours were compared to OC and BC concentrations measured.
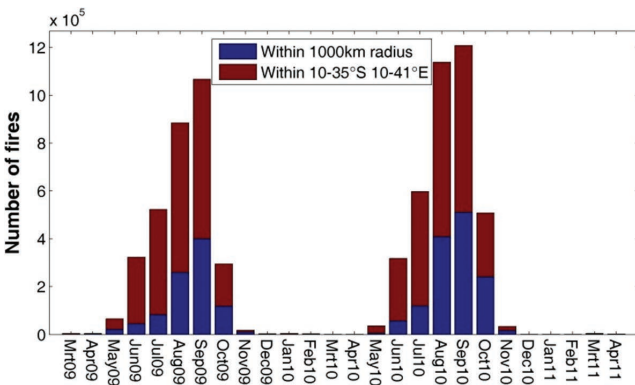
Figure 7: The frequency of biomass burning fires (obtained from MODIS burned area measurements) from March 2009 to April 2011 in southern Africa (15 – 35°S and 10 – 41°E), as well as the number of fires within a 1000 km radius from the centre of the 5 IDAF sites

(a) VT

(b) BS

(c) LT

(d) SK

(e) AF
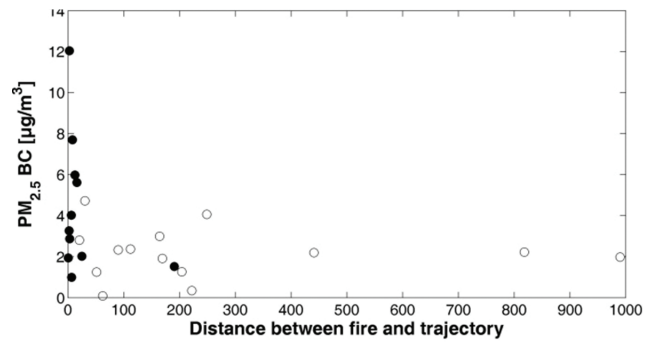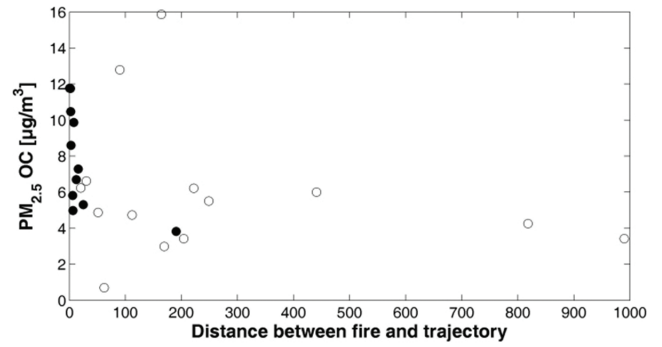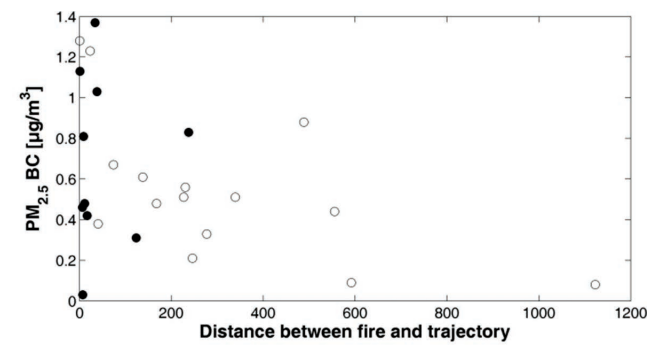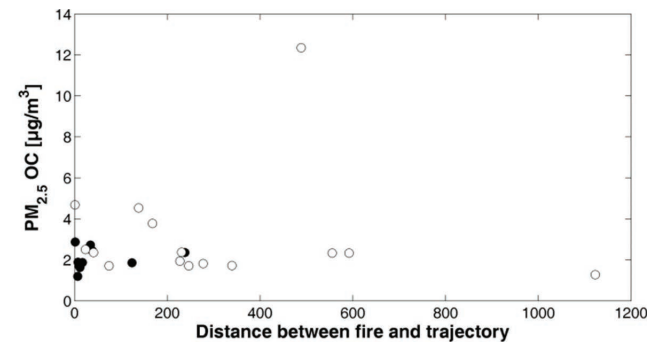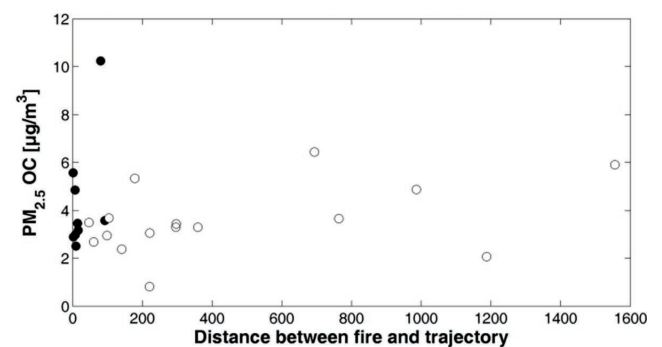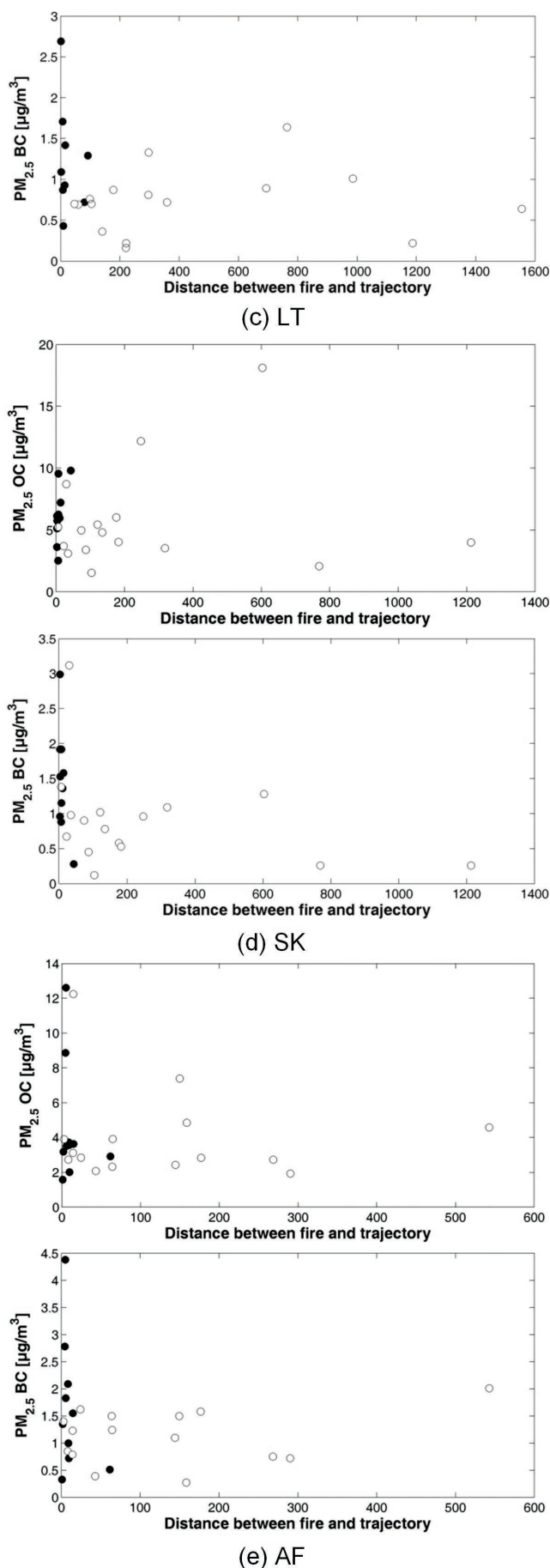
Figure 8: *$PM_{2.5}$ OC and BC concentrations plotted against the shortest distances between the back trajectories and the fire events at VT (a), BS (b), LT (c), SK (d) and AF (e). The black dots represent the months during which most fires occurred (June to October), while the open circles represent months with fewer fire events (November to May)*

In Fig. 8 OC and BC concentrations measured for $PM_{2.5}$ are plotted against the shortest distances between the 24-hour back trajectories and fire events for each sample at VT (8a), BS (8b), LT (8c), SK (8d) and AF (8e). The black dots indicated OC and BC concentrations measured during months that most fires occurred, i.e. June to October, while the open circles represent months with no or very few fire events (according to Fig. 7).

From Fig. 8 it seems that higher OC and BC concentrations were measured when trajectories passed closer to fires during the months when most fires occurred (June to October). In contrast, during the months with fewer fires (November to May), OC and BC concentrations did not seem to be influenced by the distances between the trajectories and fires. This indicates that fires are a major source of OC and BC during the months with high fire frequencies, while OC and BC measured during the other months were mainly emitted from other sources in this region. It has to be mentioned that the observed relationship, i.e. higher OC and BC contribution from biomass combustion fires during months with more fires, are somewhat obscured due to all the averaging periods in the data, i.e. 24-hour sampling, calculation of a single trajectory in the middle of the sampling period and 24-hour clustering of fire events by MODIS burned area measurements. However, a good indication of the influence of biomass burning fires during the months with high fire frequencies is obtained.

In an effort to further explore the regional contribution of biomass combustion fires to OC and BC, the data presented in Fig. 8 for individual sites were combined Fig. 9 for OC (Fig. 9a) and BC (Fig. 9b). These two figures therefore give a regional, rather than a site specific perspective of OC and BC concentrations as a function of distance to the closest fire for each calculated back trajectory. Since the VT sampling site was within an industrialised and residential region that could lead to bias in the data presentation, OC and BC measured at this sampling site were excluded from Fig. 9. Additionally the data points where the shortest distance to the fire for a specific back trajectory was >45 km were not included in this analysis (Fig. 9). Although not well defined, there seems to be a general trend between the OC and BC concentrations and the distance that a back trajectory had passed over a biomass burning fire, as indicated in Fig. 9. As previously mentioned, the reason for the scattered nature of the data in Fig. 9 can be attributed to multiple averaging periods that had to be applied, i.e. 24-hour sampling, calculation of a single trajectory in the middle of the sampling period and 24-hour grouping of fire events by MODIS burned area measurements. Notwithstanding these data limitations, it is evident that OC and BC are higher if a biomass combustion fire event(s) had impacted on a back trajectory air mass during the months with higher frequency in fire events. Therefore, fires seem to contribute significantly to both OC and

BC concentrations during the period when biomass burning fires frequently occur, i.e. June to October.

Similar to the data presented in Fig. 8, $PM_{2.5}$ OC and BC concentrations were plotted against the shortest distance that a back trajectory had passed over large anthropogenic point sources (e.g. pyrometallurgical smelters and coal-fired power stations) in the north-eastern region of South Africa, for each sampling site during every 24-hour sampling period. Thereafter, the individual datasets of SK, LT and BS were combined to give a regional, rather than a site specific perspective. The AF data was excluded since it had a large point source in close proximity to it, while VT was also excluded since it was within a source region with many large sources nearby. Data points where the distance between back trajectories and large point sources were >45 km were also not included in the analysis. The combined SK, LT and BS dataset is presented as a second data series in Fig. 9. From this data it is evident that $PM_{2.5}$ OC and BC concentrations were not influenced by the distances that back trajectories had passed over large point sources. This indicates that the contribution of these large point sources is not as significant compared to the biomass combustion fires on OC and BC concentrations. The observation that large point sources do not contribute significantly to regional BC concentrations is feasible, since emissions regulations in South Africa have historically regulated particulate emissions (which included BC) much more stringently than gaseous emissions.

(a)

(b)
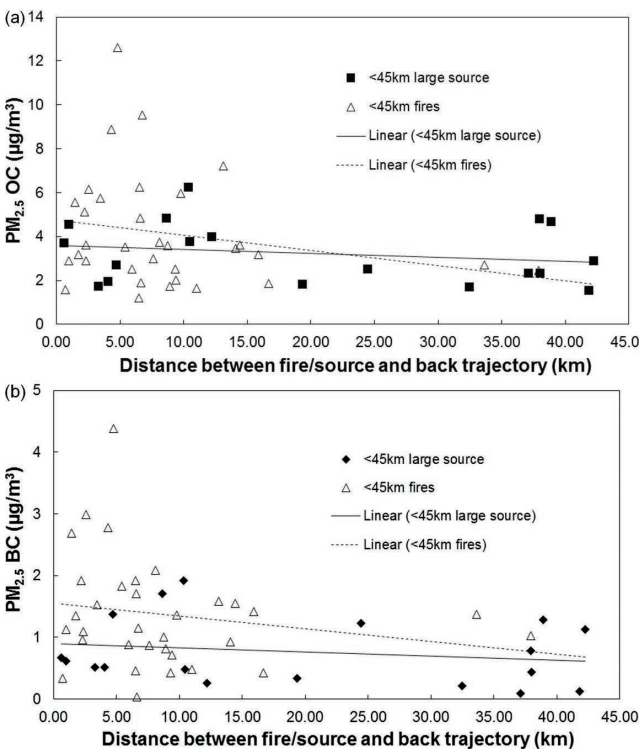
Figure 9: $PM_{2.5}$ OC (a) and BC (b) concentrations of June to October (months with higher fire frequency, according to Fig. 7) at all the sampling sites as a function of shortest distance between back trajectories and fires, excluding VT data and data where the shortest distances are >45 km. Additionally, $PM_{2.5}$ OC (a) and BC (b) concentrations of SK, LT and BS as a function of shortest distance between back trajectories and large point source, excluding data where the shortest distances are >45 km, are presented for the entire sampling period

Another possible source of OC and BC that has already been mentioned, but not yet evaluated is household combustion. Venter et al. (2012) previously suggested that household combustion in informal and semi-formal settlements in South Africa could be a significant source of BC, at least on a local scale. Household combustion generally serves two basic needs, i.e. cooking or space heating. In an effort to determine the influence of household combustion for space heating on OC and BC concentrations, the $PM_{2.5}$ OC and BC concentrations of VT were plotted against the minimum temperature measured during the actual sampling periods (Fig. 10). The VT site was specifically chosen to perform this analysis, since many informal and semi-formal settlements are present in the immediate area surrounding the measurement site.

(a)

(b)
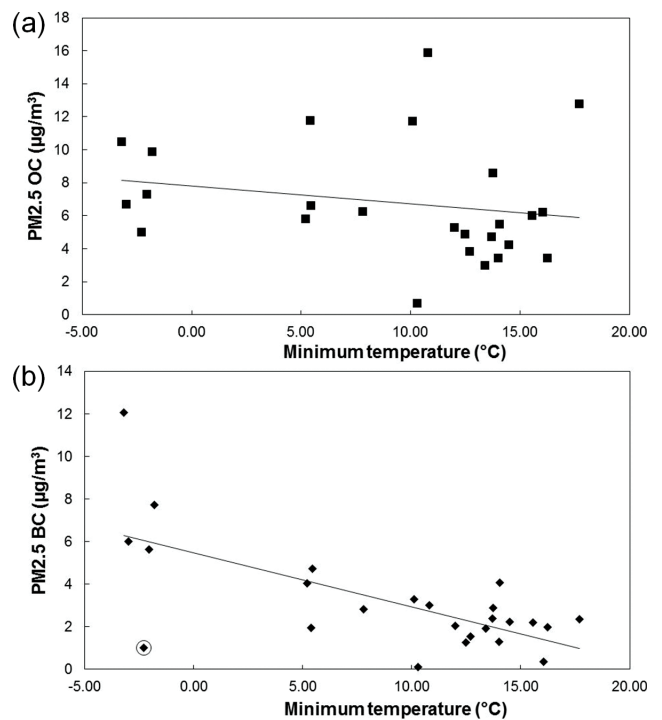
Figure 10: $PM_{2.5}$ OC (a) and BC (b) concentrations of VT plotted as a function of actual minimum temperature during the periods when the samples were collected

As is evident from Fig. 10, both $PM_{2.5}$ OC and BC concentrations seems to be inversely related to the average monthly minimum temperature. This implies that lower temperatures resulted in an increase in household combustion for space heating, which seem to result in higher OC and BC emissions. However, a weaker correlation was observed for $PM_{2.5}$ OC and minimum temperature compared to the correlation found for $PM_{2.5}$ BC and minimum temperature. This can be comprehended, since measured OC consist of primary emitted and secondary formed particles, while BC is exclusively emitted as primary particles. Therefore a better correlation between minimum temperatures and the occurrence of household combustion for space heating for BC is expected. The coefficient of determination (R^2) value for the correlation between $PM_{2.5}$ BC and minimum temperature was found to be significant, i.e. 0.45. This correlation is even more significant, i.e. 0.63, if the single circled value in Fig. 10b is excluded from the dataset.

Conclusions

The OC and BC dataset presented in this paper is one of the largest presented to date in the peer reviewed public domain for South Africa. Therefore this publication makes a contribution to a research field that is very important, e.g. BC second most important climate forcing species, but neglected. However, the dataset and methods presented here have certain limitations. Probably the most significant limitations are due to the size of the dataset and the sampling frequency. For most of the sites only one 24-hour sample per month was collected for two years and one month. This relatively small dataset makes it difficult to statistically evaluate temporal and spatial aspects, as well source contributions. Therefore the results presented should be considered as indicative and not absolute. Additionally, it also indicates the need for more comprehensive studies of this nature to be conducted. Notwithstanding the afore-mentioned limitation the following indicative deductions could be made.

OC were higher than BC concentrations at all the South African IDAF sites in the PM_{10} and $PM_{2.5}$ fractions. Most OC and BC occurred in the smaller size fraction, i.e. $PM_{2.5}$. OC and BC concentrations, as well as OC/BC ratios reflected the location of the different IDAF sites, as well as the type of sources impacting the different sites. VT, which is situated in an industrial and urban location, had the highest OC and BC concentrations with the lowest OC/BC ratio. Of the sites investigated, it was also most-likely more significantly impacted by fossil fuel combustion. AF, which is influenced by an industrial source region, had the second lowest OC/BC ratio, while the background sites (BS, LT and SK) had the highest OC/BC ratios. The background sites were also likely to be impacted by non-fossil fuel sources such as biomass burning fires. The OC and BC mass fraction percentages varied up to 24% and 12 %, respectively, for all the sites in both size fractions.

A relatively well defined seasonal pattern was observed, with higher OC and BC concentrations measured from May to October, which coincided with the dry season and highest frequency of biomass burning events in the interior of South Africa. Seasonal OC and BC mass fractions for all the sites over the entire sampling period were found to be the inverse of the seasonal OC and BC concentrations. This indicates that although OC and BC concentrations are in general higher in the dry and cold period, the atmospheric aerosol load during this period is also substantially higher, which can most-likely be attributed to wind-blown dust.

Positive correlations between OC and BC concentrations with the distance that back trajectories passed over biomass combustion fires were observed, while no such correlations were observed for the distance that back trajectories had passed over large point sources. This seems to substantiate that biomass combustion fires contribute significantly to both OC and BC concentrations on a regional scale, while this is not the case for large point sources. Correlation of OC and BC concentrations with the minimum temperatures during the sampling periods at the VT site proved that household combustion for space heating in semi- and informal settlements contributed to OC and BC levels, at least on a local scale.

References

Air Resources Laboratory. (2014a). Gridded Meteorological Data Archives. http://www.ready.noaa.gov/archives.php. Accessed 24 February 2014.

Air Resources Laboratory. (2014b). Gridded Meteorological Data Archives. http://www.arl.noaa.gov/HYSPLIT_info.php. Accessed 13 February 2014.

Air Resources Laboratory. (2014c). Gridded Meteorological Data Archives. http://www.arl.noaa.gov/faq_hg17.php. Accessed 14 February 2014.

Atkinson, R., & Arey, J. (2003). Gas-phase tropospheric chemistry of biogenic volatile organic compounds: a review. *Atmospheric Environment*, 37(2), S197-S219. doi: 10.1016/S1352-2310(03)00391-1.

Baldauf, R.W., Lane, D.D., Marotz, G.A., & Wiener, R.W. (2001). Performance evaluation of the portable MiniVOL particulate matter sampler. *Atmospheric Environment*, 35, 6087-6091. PII: S1352-2310(01)00403-4.

Beukes, J.P., Vakkari, V., Van Zyl, P.G., Venter, A.D., Josipovic, M., Jaars, K., Tiita, P., Siebert, S., Pienaar, J.J., Kulmala, M., & Laakso, L. (2013). Welgegund - long-term land atmosphere measurement platform in South Africa. iLeaps Newsletter. *Integrated Land Ecosystem Atmosphere Process Study*, 12, 24-25.

Bond, T.C., & Sun, H. (2005). Can Reducing black carbon emission counteract global warming? *Environmental Science and Technology*, 39, 5921-5926.

Cachier, H., Auglagnier, F., Sarda, R., Gautier, F., Masclet, P., Besombes, J.-L., Marchand, N., Despiau, S., Croci, D., Mallet, M.,Laj, P., Marinoni, A., Deveau, P.-A., Roger, J.-C., Putaud, J.-P., Van Dingenen, R., Dell'Acqua, A., Viidanoja, J., Martins-Dos Santos, S., Liousse, C., Cousin, F., Rosset, R. Gardrat, E., & Galy-Lacaux, C. (2005). Aerosol studies during the ESCOMPTE experiment: An overview. *Atmospheric Research*, 74:547-563. doi: 10.1016/j.atmosres.2004.06.013.

Chazette, P., & Liousse, C. (2001). A case study of optical and chemical ground apportionment for urban aerosols in Thessaloniki. *Atmospheric Environment*, 35, 2497-2506. PII: S1352-2310(00)00425-8.

Chow, J.C., Watson, J.G., Crow, D., Lowenthal, D.H., & Merrifield, T. (2001). Comparison of IMPROVE and NIOSH carbon measurements. *Aerosol Science and Technology*, 34, 23-24.

Chow, J.C., Watson, J.G., Kuhns, H., Etyemezian, V., Lowenthal, D.H., Crow, D., Kohl, S.D., Engelbrecht, J.P., & Green, M.C. (2004). Source profiles for industrial, mobile, and area sources in the Big Bend Regional Aerosol Visibility and Observational study. *Chemosphere*, 54, 185-208.

Chow, J.C., Watson, J.G., Pritchett, L.C., Pierson, W.R., Frazier, C.A., & Purcell, R.G. (1993). The dri thermal/optical reflectance carbon analysis system: description, evaluation and applications in U.S. Air quality studies. *Atmospheric Environment, Part A General Topics*, 27(8), 1185-1201.

Collett, K.S., Piketh, S.J., & Ross, K. E. (2010). An assessment of the atmospheric nitrogen budget on the South African Highveld. S*outh African Journal of Science*, 106(5/6), 1-9. doi: 10.4102/sajs.v106i5/6.220.

de Richter, R., & Caillol, S. (2011). Fighting global warming: The potential of photocatalysis against CO_2, CH_4, N_2O, CFCs, tropospheric O_3, BC and other major contributors to climate change. *Photochemistry and Photobiology*, 12, 1-19. doi: 10.1016/j.jphotochemrev.2011.05.002.

Doumbia, E.H.T., Liousse, C., Galy-Lacaux, C., Ndiaye, S.A., Diop, B., Ouafo, M., Assamoi, E.M., Gardrat, E., Castera, P., Rosset, R., Akpo, A., & Sigha, L. (2012). Real time black carbon measurements in West and Central Africa urban sites. *Atmospheric Environment*, 54, 529-537. doi: 10.1016/j.atmosenv.2012.02.005.

Draxler, R. R., & Hess, G. D. (2004). *Description of the HYSPLIT 4 Modelling System, NOAA Technical Memorandum ERL* ARL-224.

Environmental analysis facility. (2008). DRI Standard operating procedure. 86p. Laboratoired'Aérologie – UMR 5560. http://www.aero.obs-mip.fr/spip.php?article489. Accessed 18 July 2011.

Formenti, P., Elbert, W., Maenhaut, W., Haywood, J., Osborne, S., & Andreae, M.O. (2003). Inorganic and carbonaceous aerosols during the Southern African Regional Science Initiative (SAFARI 2000) experiment: Chemical characteristics, physical properties, and emission data for smoke from African biomass burning. *Journal of geophysical Research*, 108, D13:8488. doi: 10.1029/2002JD002408.

Galy-Lacaux, C., Al Ourabi, H., Lacaux, J.-P., Pont, V., Galloway, J., Mphepya, J., Pienaar, K., Sigha, L., & Yoboué, V. (2003). Dry and wet atmospheric nitrogen deposition in Africa. *IGAC Newsletter*, January 2003, Issue nr. 27, 6-11.

Gauderman, W.J., Avol, E., Gilliland, F., Vora, H., Thomas, D., Berhane, K., Mcconnell, R., Kuenzli, N., Lurmann, F., Rappaport, E., Margolis, H., Bates, D., & Peters, J. (2004). The effect of air pollution on lung development from 10 to 18 years of age. *The New England Journal of Medicine*, 351(11), 1057-1067.

Government Gazette Republic of South Africa, 14 October 2005, No. 28132.

Guillame, B., Liousse, C., Galy-Lacaux, C., Rosset, R., Gardrat, E., Cachier, H., Bessagnet, B., & Poisson, N. (2008). Modeling exceptional high concentrations of carbonaceous aerosols observed at Pic du Midi in spring-summer 2003: Comparison with Sonnblick and Puy de Dôme. *Atmospheric Environment*, 42, 5140-5149. doi: 10.1016/j.atmosenv.2008.02.024.

HYSPLIT User's Guide-Version 4. Last revised: April 2013. http://www.arl.noaa.gov/documents/reports/hysplit_user_guide.pdf. Accessed 13 February 2014.

Hyvärinen, A.-P., Vakkari, V., Laakso, L., Hooda, R.K., Sharma, V.P., Panwar, T.S., Beukes, J.P., Van Zyl, P.G., Josipovic, M., Garland, R.M., Andreae, M.O., Pöschl, U., & Petzold, A. (2013). Correction for a measurement artifact of the Multi-Angle Absorption Photometer (MAAP) at high black carbon mass concentration levels. *Atmospheric Measurement Techniques*, 6, 81-90. doi: 10.5194/amt-6-81-2013.

IPCC (Intergovernmental Panel For Climate Change). (2013). *IPCC fifth assessment report: Climate change 2013*.

Jaars, K., Beukes, J.P., Van Zyl, P.G., Venter, A.D., Josipovic, M., Pienaar, J.J., Vakkari, V., Aaltonen, H., Laakso, H., Kulmala, M., Tiitta, P., Guenther, A., Hellén, H., Laakso. L., & Hakola, H. (2014). Ambient aromatic hydrocarbon measurements at Welgegund, South Africa. *Atmospheric Chemistry and Physics*, 14, 4189-4227. doi: 10.5194/acpd-14-4189-2014.

Junker, C., & Liousse, C. (2008). A global emission inventory of carbonaceous aerosol from historic records of fossil fuel and biofuel consumption for the period 1860-1997. *Atmospheric Chemistry and Physics*, 8, 1195-1207. www.atmos-chem-phys.net/8/1195/2008/. Accessed 10 March 2014.

Kanakidou, M., Seinfeld, J.H., Pandis, S.N., Barnes, I., Dentener, F.J., Facchini, M.C., Van Dingenen, R., Ervens, B., Nenes, A., Nielson, C.J., Swietlicki, E., Putaud, J.P., Balkanski, Y., Fuzzi, S., Horth, J., Moortgat, G.K., Winterhalter, R., Myhre, C.E.L., Tsigaridis, K., Vignati, E., Stephanou, E.G., & Wilson, J. (2005). Organic aerosol and global climate modelling: a review. *Atmospheric chemistry and Physics*, 5, 1053-1123. SRef-ID: 1680-7324/acp/2005-5-1053.

Laakso, L., Vakkari, V., Virkkula, A., Laakso, H., Backman, J., Kulmala, M., Beukes, J.P., van Zyl, P.G., Tiitta, P., Josipovic,

M., Pienaar, J.J., Chiloane, K., Gilardoni, S., Vignati, E., Wiedensohler, A., Tuch, T., Birmili, W., Piketh, S., Collett, K., Fourie, G.D., Komppula, M., Lihavainen, H., de Leeuw, G., & Kerminen, V.-M. (2012). South African EUCAARI measurements: seasonal variation of trace gases and aerosol optical properties. *Atmospheric Chemistry and Physics*, 12, 1847–1864. doi: 10.5194/acp-12-1847-2012.

Lazaridis, M., Semb, A., Larssen, S., Hjellbrekke, A.-G., Hov, Ø., Hanssen, J.E., Schaug, J., & Tørseth, K. (2002). Measurements of particulate matter within the framework of the European Monitoring and Evaluation Programme (EMEP) I. First results. *The Science of the Total Environment*, 285, 209-235. PII: S0048-9697(01)00932-9.

Liousse, C., Penner, J.E., Chuang, C., Walton, J.J., Eddleman, H., & Cachier,H. (1996). A global three-dimensional model study of carbonaceous aerosols. *Journal of Geophysical Research*, 105, 26871-26890.

Lourens, A.S.M., Beukes, J.P., van Zyl, P.G., Fourie, G.D., Burger, J.W., Pienaar, J.J., Read, C.E., & Jordaan, J.H.L. (2011). Spatial and Temporal assessment of Gaseous Pollutants in the Mpumalanga Highveld of South Africa. South African Journal of Science, 107(1/2), 8. Art. #269. doi: 10.4102/sajs.v107i1/2.269.

Lourens, A.S.M., Butler, T.M., Beukes, J.P., Van Zyl, P.G., Beirle, S., Wagner, T.K., Heue, K.-P., Pienaar, J.J., Fourie, G.D., & Lawrence, M.G. (2012). Re-evaluating the NO_2 hotspot over the South African Highveld. *South African Journal of Science*, 108(11/12). http://dx.doi.org/10.4102/sajs.v108i11/12.1146. Accessed 10 March 2014.

Martins, J.J. (2009). *Concentrations and deposition of atmospheric species at regional sites in southern Africa*. M.Sc. NWU Potchefstroom. 224p.

Martins, J.J., Dhammapala, R.S., Lachmann, G., Galy-Lacaux, C., & Pienaar, J.J. (2007). Long-term measurements of sulphur dioxide, nitrogen dioxide, ammonia, nitric acid and ozone in southern Africa using passive samplers. *South African Journal of Science*, 103, 336-342.

MODIS: Obtaining and processing MODIS data. http://www.yale.edu/ceo/Documentation/MODIS_data.pdf. Accessed 14 February 2014.

Mphepya, J.N., Galy-Lacaux, C., Lacaux, J.P., Held, G., & Pienaar, J.J. (2006). Precipitation Chemistry and Wet Deposition in Kruger National Park, South Africa. *Journal of Atmospheric Chemistry*, 53, 169-183. doi: 10.1007/s10874-005-9005-7.

Mphepya, J.N., Pienaar, J.J., Galy-Lacaux, C., Held, G., & Turner, C.R. (2004). Precipitation Chemistry in Semi-Arid Areas of Southern Africa: A Case Study of a Rural and an Industrial Site. *Journal of Atmospheric Chemistry*, 47, 1-24.

Mucina, L., & Rutherford, M.C. eds. (2006). *The vegetation of South Africa, Lesotho and Swaziland*. Strelitzia 19. Pretoria: South African National Biodiversity Institute. 807p.

Nasa. (2015) http://gcmd.nasa.gov/records/ GCMD_gov.noaa.ncdc.C00075.html. Accessed 28 April 2015.

Oberdőrster, G., Sharp, S., Atudorei, V., Elder, A., Gelein, R., Kreyling, W., & Cox, C. (2004). Translocation of inhaled ultrafine particles to the brain. *Inhalation toxicology*, 16, 437-445. doi: 10.1080/08958370490439597.

Pöschl, U. (2005). Atmospheric Aerosols: Composition, Transformation, Climate and Health Effects. Atmospheric Chemistry: Reviews. *Angew. Chem. Int*. Ed, 44, 7520-7540. doi: 10.1002/anie.200501122.

Putaud, J.-P., Raes, F., Van Dingenen, R., Brűggemann, E., Facchini, M.-C., Decesari, S., Fuzzi, S., Gehrig, R., Hűglin, C., Laj, P., Lorbeer, G., Maenhaut, W., Mihalopoulos, N., Műller, K., Querol, X., Rodriguez, S., Schneider, J., Spindler, G., Ten Brink, H., Tørseth, K., & Wiedensohler, A. (2004). A European aerosol phenomenology-2: chemical characteristics of particulate matter at kerbside, urban, rural and background sites in Europe. *Atmospheric Environment*, 38, 2579-2595. doi: 10.1016/j.atmosenv.2004.01.041.

Riddle, E.E., Voss, P.B., Stohl, A., Holcomb, D., Maczka, D., Washburn, K., & Talbot, R.W. (2006). Trajectory model validation using newly developed altitude-controlled balloons during the International Consortium for Atmospheric Research on Transport and Transformations 2004 campaign. *Journal of Geophysical Research*, 111, D23S57. doi: 10.1029/2006JD007456.

Roy, D.P., Boschetti, L., Justice, C.O., & Ju, J. (2008). The collection 5 MODIS burned area product-Global evaluation by comparison with the MODIS active fire product. *Remote Sensing of Environment*, 112, 3690-3707p. doi: 10.1016/j.rse.2008.05.013.

Seinfeld, J. H., & Pandis, S. N. (2006). A*tmospheric Chemistry and Physics: From Air Pollution to Climate Change*. John Wiley & Sons Inc.

Slanina, S., & Zhang, Y. (2004). Aerosols: Connection between regional climatic change and air quality. IUPAC. *Pure and applied chemistry*, 76(6), 1241-1253.

Stohl, A. (1998). Computation, accuracy and application of trajectories – a review and bibliography. *Atmospheric Environment*, 32, 947–966.

Swap, R.J., Aranibar, J.N., Dowty, P.R., Gilhooly (III), W.P., & Macko, S.A. (2004). Natural abundance of ^{13}C and ^{15}N in C3 and C4 vegetation of southern Africa: patterns and implications. *Global Change Biology*, 10, 350-358. doi: 10.1046/j.1529-8817.2003.00702.x.

Tiitta, P_.,Vakkari, V., Croteau, P., Beukes, J.P., Van Zyl, P.G., Josipovic, M., Venter, A.D., Jaars, K., Pienaar, J.J., Ng, N.L., Canagaratna, M.R., Jayne, J.T., Kerminen, V.-M., Kokkola, H., Kulmala, M., Laaksonen, A., Worsnop, D.R., & Laakso, L. (2014). Chemical composition, main sources and temporal variability of PM_1 aerosols in southern African grassland. *Atmospheric Chemistry and Physics*, 14, 1909–1927. doi: 10.5194/acp-14-1909-2014.

Tummon, F., Solmon, F., Liousse, C., & Tadross, M. (2010). Simulation of the direct and semidirect aerosol effects on the southern Africa regional climate during the biomass burning season. *Journal of Geophysical Research D: Atmospheres*, 115(19). Art. no. D19206.

Tyson, P.D., & Preston-Whyte, R.A. (2000). *The Weather and Climate of Southern Africa*. Oxford University Press. South Africa. 396p. VK551.50968TYS

Val, S., Liousse, C., Doumbia, E.H.T., Galy-Lacaux, C., Cachier, H., Marchand, N., Badel, A., Gardrat, E., Sylvestre, A., & Baeza-Squiban, A. (2013). Physico-chemical characterization of African urban aerosols (Bamako in Mali and Dakar in Senegal) and their toxic effects in human bronchial epithelial cells: description of a worrying situation. *Particle and Fibre Toxicology*, 10, 10.

Vakkari, V., Kerminen, V.-M., Beukes, J. P., Tiitta, P., Van Zyl, P.G., Josipovic, M., Venter, A.D., Jaars, K., Worsnop, D.R., Kulmala, M., & Laakso, L. (2014). Rapid changes in biomass burning aerosols by atmospheric oxidation. *Submitted to Geophysical Research Letters*.

Vakkari, V., Laakso, H., Kulmala, M., Laaksonen, A., Mabaso, D., Molefe, M., Kgabi, N., & Laakso, L. (2011). New particle formation events in semi-clean South African savannah. *Atmospheric Chemistry and Physics*, 11, 3333-3346.

Venter, A.D., Vakkari, V., Beukes, J.P., Van Zyl, P.G., Laakso, H., Mabaso, D., Tiitta, P., Josipovic, M., Kulmala, M., Pienaar, J.J., & Laakso, L. (2012). An air quality assessment in the industrialised western Bushveld Igneous Complex, South Africa. *South African Journal of Science*, 10(9/10). http://dx.doi.org/10.4102/sajs.v108i9/10.1059. Accessed 10 March 2014.

Yin, J., Allen, A.G., Harrison, R.M., Jennings, S.G., Wright, E., Fitzpatrick, M., Healy, T., Barry, E., Ceburnis, D., & McCusker, D. (2005). Major component of urban PM_{10} and $PM_{2.5}$ in Ireland. *Atmospheric Research*, 78, 149-165. doi: 10.1016/jatmosres.2005.03.006.

Zhang, Q., Jimenez, J.L., Canagaratna, M.R., Allan, J.D. Coe, H., Ulbrich, I., Alfarra, M.R., Takami, A., Middlebrook, A.M., Sun, Y.L., Dzepina, K., Dunlea, E., Docherty, K., DeCarlo, P.F., Salcedo, D., Onasch, T., Jayne, J.T. Miyoshi, T., Shimono, A., Hatakeyama, S., Takegawa, N., Kondo, Y., Schneider, J., Drewnick, F., Borrmann, S., Weimer, S., Demerjian, K., Williams, P., Bower, K., Bahreini, R., Cottrell, L., Griffin, R.J., Rautiainen, J., Sun, J.Y., Zhang, Y.M., &

Worsnop, D.R. (2007). Ubiquity and dominance of oxygenated species in organic aerosols in anthropogenically-influenced Northern Hemisphere midlatitudes. *Geophysical Research Letters*, 34, L13801. doi: 10.1029/2007GL029979.